phys. stat. sol. (a) **168**, 309 (1998)

Subject classification: 78.66.Hf; 71.35.Cc; 78.45.+h; S8.12; S8.15

Optical Properties and Lasing in CdSe-Submonolayers in a (Zn,Mg)(S,Se) Matrix

I. L. KRESTNIKOV[1]) (a), N. N. LEDENTSOV[2]) (a), A. HOFFMANN (a), D. BIMBERG (a), S. V. IVANOV (b), M. V. MAXIMOV (b), A. V. SAKHAROV (b), S. V. SOROKIN (b), P. S. KOPEV (b), ZH. I. ALFEROV (b), and C. M. SOTOMAYOR TORRES (c)

(a) Institut für Festkörperphysik, Technische Universität Berlin, Hardenbergstraße 36, D-10623 Berlin, Germany

(b) A. F. Ioffe Physico-Technical Institute, Russian Academy of Sciences, Polytekhnicheskaya 26, 194021 St.-Petersberg, Russia

(c) Lehrstuhl für Materialwissenschaften in der Elektrotechnik, Bergische Universität GH Wuppertal, Fuhlrottstraße 10, D-42097 Wuppertal, Germany

(Received January 19, 1998; in revised form March 20, 1998)

We have proposed and realized a new type of optoelectronic structures we refer to as *excitonic waveguides* which allow an ultimate shift towards the violet spectral range (460 nm at 300 K for the ZnMgSSe/GaAs materials system). The excitonic waveguiding effect is realized at the low energy side of the strong exciton absorption peak due to localized states, caused by ultrathin narrow-gap insertions. To realize the zero-phonon lasing mechanism resonant to the spectral region of resonantly enhanced refractive index one needs to break the *k*-selection rule preventing direct radiate exciton recombination having large in-plane *k*-vector dominating at high excitation densities and observation temperatures. This can be done by localizing excitons at nanoscale CdSe-rich islands formed by ultrathin CdSe insertions.

1. Introduction

Up to now the structure of wide-bandgap lasers is similar to that for conventional infrared III–V lasers, in general agreement with the double-heterostructure laser geometry [1]. The using of thick layers of wider bandgap material having a lower refractive index is assumed to be necessary. However, this wider bandgap material, lattice matched to the active layer does not necessary exist for each particular case, or, if exists, does not necessarily provide sufficient conductivity. Moreover, interest in ultimate shift towards blue and UV spectral regions requires in any case an alternative approach for efficient waveguiding. An attractive idea is to use the effect of resonant enhancement of the refractive index which arises on the low energy side of the absorption peak as it follows from Kramers-Kronig equations which relate real and imaginary parts of the dielectric susceptibility.

A natural condidate for resonant absorption is the exciton absorption in bulk and in quantum wells (QWs). In conventional narrow gap III–V QWs, however, excitons are

[1]) Corresponding author. Tel.: +7 812 247 9124, Fax: +7 812 247 8640, e-mail: igor@beam.ioffe.rssi.ru

[2]) On leave from Ioffe Institute.

effectively screened by carriers upon injection resulting in bleaching of the exciton absorption. As opposite, high exciton binding energies and oscillator strength and high densities required to screen excitons in II–VI and III–V materials (around 10^{19} cm^{-3}) make the resonant excitonic absorption an attractive candidate to realize this type of waveguides [2]. At the same time, however, the exciton-induced lasing, resonant to the range of the strongly enhanced refractive index, can be hardly realized in bulk wide-gap II–VI compounds. Free excitons with finite k-values dominating at high excitation densities and observation temperatures cannot recombine radiatively, as it was demonstrated first by Gross et al. [3], and an additional particle (LO-phonon) is necessary to accomodate the exciton k-vector. Thus, gain appears to be shifted away from the waveguiding region by at least one LO-phonon energy. To overcome this problem one needs to propose a mechanism leading to lifting of the k-selection rule.

In this sense arrays of stacked quantum dots (QDs) represent an attractive case for the realization of the idea as the screening effect is much less important in this case and the zero-phonon exciton or biexciton lasing can be realized. Ultrahigh exciton oscillator strength in QDs allows to achieve strong resonant absorption even in case of very diluted arrays of QD, thus making possible the realization of rather thick dislocation-free active regions with thickness comparable to the lightwave in the crystal. These unique properties make the QD excitonic waveguides applicable for lasers both in III to V and II–VI materials system. More recently, submonolayer (SML) insertions were proposed to be used in excitonic waveguides [4]. Due to exciton localization at islands formed by SML deposition, the structures composed of stacked SMLs result both in lifting of k-selection rule and in a giant increase in the exciton oscillator strength, indeed providing a new possibility for lasing and waveguiding in wide bandgap matrices.

2. Growth and Experimental Procedures

The structures extensively studied in this work were grown on n^+ GaAs(100) substrates using molecular beam epitaxy (MBE). The details of MBE growth and composition control of lattice-matched quaternary and ternary (Zn,Mg)(S,Se) alloys have been described elsewhere [5]. Structures A and B were grown at $T_S = 295$ and 270 °C, respectively. The structures comprised a 20 nm thick ZnSe buffer layer grown on the substrate followed by a 1300 nm thick $ZnS_{0.06}Se_{0.94}$ layer (structure A) or by a 850 nm thick $Zn_{0.92}Mg_{0.08}S_{0.13}Se_{0.87}$ layer (structure B). After that, an active region was grown. First, a 10 nm thick wider bandgap ZnMgSSe barrier was grown to prevent carrier spreading into the lower layer and the GaAs substrate. This layer was followed a submonolayer superlattice (SML SL) confined on both sides by 50 nm ZnSSe layers (structure A) or ZnMgSSe layers (structure B). A 10 nm thick top barrier layer was deposited to prevent surface recombination. SML SL composed of 20 periods of 1/2 monolayer (ML) CdSe insertions separated by 3 nm thick ZnSe layers (structure A) or ZnMgSSe layer (structure B). The SML SLs were grown in conventional MBE growth mode with several second long exposure under Se flux at each of the interfaces in the SL.

Photoluminescence (PL), optical reflection (OR) and lasing spectra were recorded using a temperature-controlled closed-cycle He cryostat. Either the 325 nm line of a He–Cd laser (3 mW) or the light from a halogen lamp were used as excitation for PL and OR spectra, respectively. For the high excitation density measurements a N_2 pulsed laser was used. To realize stripe excitation the laser beam was focused using a cylindrical lens.

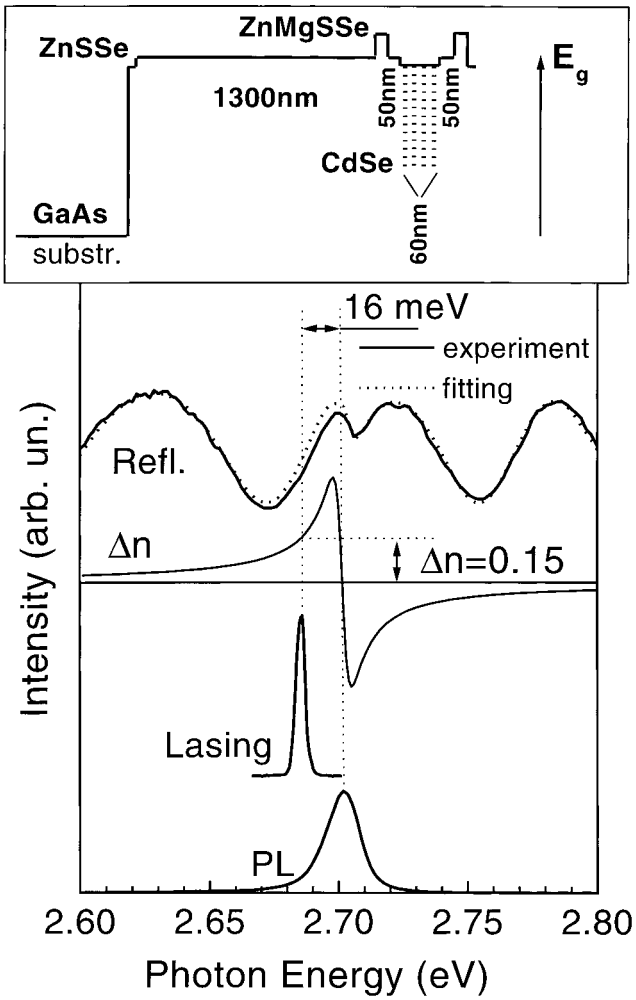

Fig. 1. Photoluminescence (PL), lasing, optical reflectance (OR) and OR fitting spectra of the structure A with submonolayer superlattice (SML SL). The values of the refractive index enhancement (Δn) calculated assuming isotropic media is also shown. The schematic bandgap diagram of the structure A is presented on top

3. Results and Discussion

In Fig. 1 we show PL, OR and lasing spectra of the structure A measured at 80 K. The peak of the PL originates from the recombination of excitons confined by the CdSe islands. As it follows from high-resolution transmission electron microscopy, the lateral size of the islands is about 4 to 5 nm [6]. The exciton confinement is caused by the fact that CdSe has a smaller bandgap (1.8 eV) as compared to the matrix material (2.8 eV). On the other hand, strong size quantization effects for carriers in the ultrathin islands result in luminescence energies close to the bandgap of the matrix. As the lateral size of the island (4 to 5 nm) [6] is comparable to the exciton diameter in ZnSe, lateral localization of the exciton wavefunction has to be rather efficient. As it foolows from Fig. 1 the OR spectrum exhibits significant modulations. The strongest modulations which is quasi-periodic in a wavelength scale is the result of the interference effect in the Fabry-Pérot resonator formed by structure/air and substrate/structure interfaces.

This modulation is typical for all A^2B^6 structures grown on a GaAs substrate. The period agrees fairly well with the results of numerical simulation of the OR spectrum described below. The remarkable result which follows from Fig. 1 is an extremely pronounced modulation of the OR spectra at the SML SL heavy-hole exciton energy (2.70 eV), which indicates a strongly enhanced exciton oscillator strength and, hence, an effective refractive index modulation due to stacked submonolayer insertions. As it was pointed out theoretically in [7], ultrahigh exciton oscillator strength, can be realized even in very diluted arrays of QDs (several percent of the surface coverage). To fit the OR spectrum we used a transfer matrix technique according to the model which included five layers: semi-infinite air layer ($n = 1$), 60 nm thick ZnSSe cap layer, 60 nm thick SML SL, 1400 nm thick ZnSSe and semiinfinite GaAs substrate ($n = 4.5$, $\alpha = 1.5 \times 10^5\ \mathrm{cm}^{-1}$). We used the following dependence of the refractive index value on photon energy for all the A^2B^6 layers [8]:

$$n_b^2(\hbar\omega) = A + \frac{B}{1 - C(\hbar\omega - \Delta)^2}\,, \tag{1}$$

where A, B and C have values 5.362, 0.7822 and 0.1044 eV^{-2}, respectively, and Δ is the bandgap difference between ZnSe and ZnSSe ($\Delta = 0.045$ eV for second and fourth layers). To describe the QD exciton peculiarity in the OR spectrum we assume a resonant dependence of the dielectric constant in the region of the SML SL [9],

$$\varepsilon(\hbar\omega) = \varepsilon_b(\hbar\omega)\left(1 + \frac{\hbar\omega_{LT}}{\hbar\omega_0 - \hbar\omega - i\hbar\Gamma}\right), \tag{2}$$

where ε_b is the background dielectric constant ($\varepsilon_b = n_b^2$); $\hbar\omega_0$, $\hbar\omega_{LT}$, $\hbar\Gamma$ are the exciton resonance, longitudinal–transverse splitting and damping energies, respectively. Fitting of the calculated OR spectrum to experimental data gives the following values for those energies: $\hbar\omega_0 = 2.701$ eV, $\hbar\omega_{LT} = 1.9$ meV and $\hbar\Gamma = 3.5$ meV. The spectral region of the exciton-induced enhancement of the refractive index and, thus, of the exciton-induced waveguiding is placed to the low-energy side from the exciton resonance energy [2]. The antiwaveguiding region is, consequently, placed to the high energy side of this energy. As follows from Fig. 1, the lasing spectrum recorded from the cleavage of the structure is 16 meV Stokes shifted towards lower energies with respect to the PL peak recorded from the surface and the exciton resonance energy in the OR spectrum. The calculated dependence of the refractive index enhancement also presented in Fig. 1, can be evaluated from the spectral dependence of the dielectric constant ($\Delta n(\omega) = \mathrm{Re}\sqrt{\varepsilon(\omega)} - \sqrt{\varepsilon_b}$). From the figure one can see that the refractive index enhancement at the lasing wavelength is about 0.15. This value is comparable with the refractive index enhancement provided by thick ZnMgSSe cladding layers if those would be introduced. We assumed here that the refractive index is isotropic within the waveguiding region, for simplicity. This assumption is valid for QDs having a spherical or cubic shape, where the quantized k-values of heavy and light holes are similar in all three directions. For QDs having a two-dimensional shape (flat islands), according to the Kane matrix elements, the oscillator strength for heavy hole exciton for the light propagating parallel to the surface (TE polarization) should be twice larger than those measured from the surface [10], and the refractive index enhancement should be, thus, also twice larger. Thus, the values of the resonant refractive index enhancement presented in Fig. 1 give a lower estimate, while the more realistic value can be

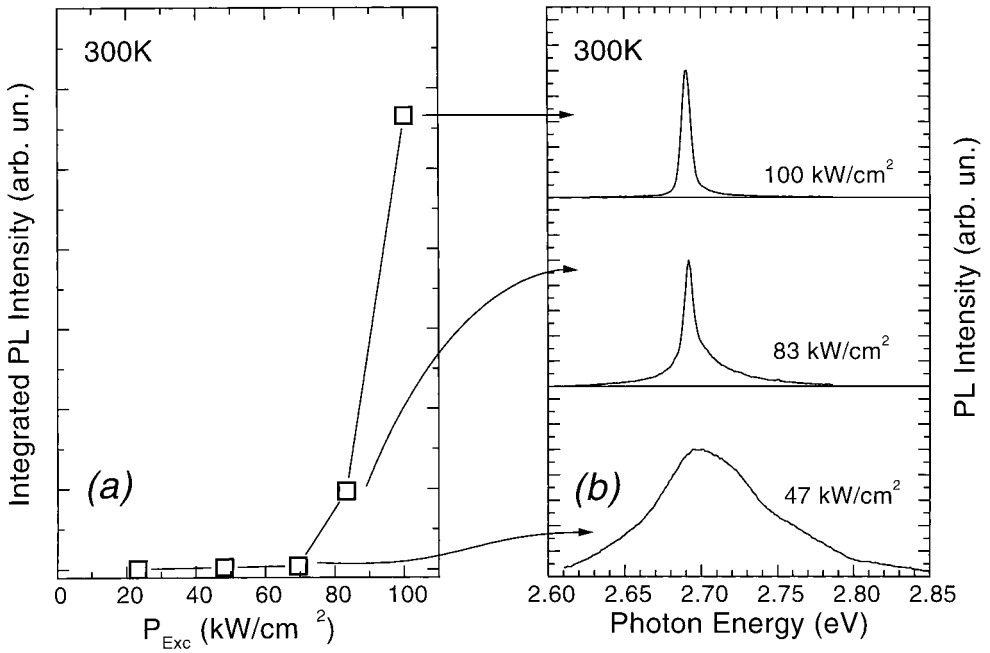

Fig. 2. Dependence of the integrated PL intensity vs. a) excitation density and b) emission spectra for several excitation densities

derived in absorption/gain studies performed in waveguide geometry which are under way now.

$ZnS_{0.06}Se_{0.94}$–$Zn_{0.8}Cd_{0.2}Se$ quantum well laser structures lase at energies $\approx\hbar\omega_{LO}$ (30 meV) below the exciton transition revealed by PL and OR spectra, in agreement with the exciton–LO phonon gain mechanism [11, 12] briefly described above. In the SML SL case, the exciton localization makes the interaction with another particle (LO-phonon, or another exciton) unnecessary, allowing the lasing to occur without additional manybody interactions in the region of the exciton-induced waveguiding.

In structure B, the bandgap of the matrix material is larger than in structure A. As the island material is the same this results in a larger exciton localization energy. It allows us to realize lasing up to room temperature. Fig. 2a demonstrates the dependence of integral PL intensity at 300 K versus excitation density recorded for structure B. The emission spectra are shown in Fig. 2b for several excitation densities. Lasing threshold is clearly demonstrated by the characteristic increase in differential efficiency with increase in the excitation density (Fig. 2a) and by the respective narrowing of the emission spectrum. Lasing action is also confirmed by the appearance of sharp lasing modes revealed in samples with small cavity lengths. One should specially note that the lasing wavelength is as low as 460 nm ($\approx$2.7 eV) in the structure with the bandgap energy of the matrix $E_g = 2.86$ eV at 300 K.

Fig. 3 demonstrates the dependence of the threshold excitation density (P_{th}) versus the stripe length (L) at 16 K. As it was shown in [13, 14] P_{th} is related to L as

$$P_{th} = \text{const}\left[(\Gamma\beta J_0 + \alpha_{int}) + \frac{1}{L}\ln\left(\frac{1}{R}\right)\right], \tag{3}$$

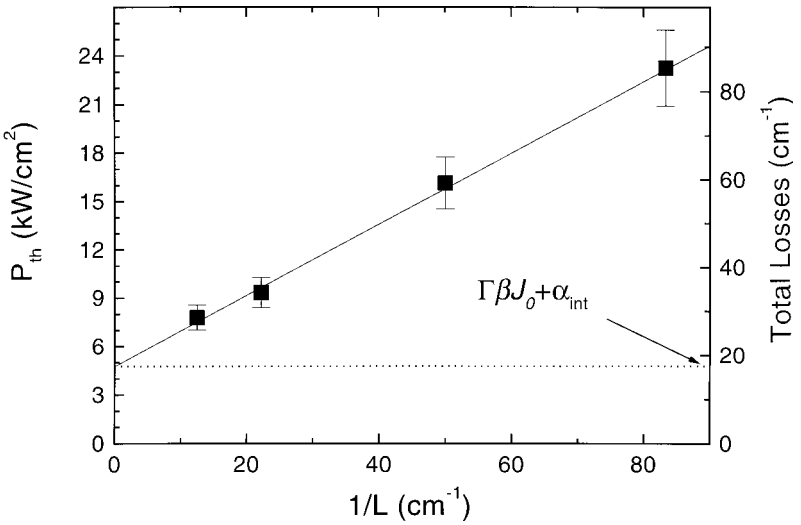

Fig. 3. Dependence of the threshold excitation density vs. stripe length

where Γ is the confinement factor of the light, β is the gain constant, J_0 is the nominal current density, α_{int} is the internal loss and R is the reflectance of cleaved facet mirrors. R is calculated from the refractive index of ZnMgSSe at lasing wavelength giving $\ln(1/R) = 0.81$. From the slope of P_{th} versus L^{-1} shown in Fig. 3 one can obtain $[\Gamma\beta J_0 + \alpha_{\text{int}} = 18\,\text{cm}^{-1}]$. Thus, the internal losses (α_{int}) in structure B are less than $18\,\text{cm}^{-1}$. These values of internal losses are comparable with the values estimated in our structures with thick ZnMgSSe cladding layers, where optical confinement is provided by thick wider bandgap layers with small refractive index [13]. Additionally, we have fabricated and studied CdSe–ZnSe SML SL structures grown in ZnSSe buffer layers as thin as 0.3 μm and also realized zero-phonon lasing, and even for the spacer layer thickness of 8 nm (i.e. in very diluted arrays of CdSe QDs $\bar{X}_{\text{Cd}} \approx 2.5\%$). This shows that the enhancement in n is rather high in this case as well and entirely exciton-induced waveguiding and lasing can be obtained also for ultrathin injectors and/or very diluted island concentrations.

4. Conclusions

Short wavelength lasing in the spectral region of the exciton-induced enhancement of the refractive index (460 nm at 300 K) is realized in the structure with 20-period SML SL. The effect of exciton-induced waveguiding, responsible for this lasing, can be also usefull to achieve lasing in materials where no lattice-matched heteropair is available, e.g. for III–V quantum dots in a silicon matrix, in diamond, etc. This effect can also help to realize the ultimately short wavelength limit for lasing in II–VI and group III nitride structures.

Acknowledgements This work was supported by the Russian Foundation of Basic Research (Grant No. 97-02-18138), by the INTAS 94-481 and by the Volkswagen Foundation. N. N. Ledentsov is grateful to the Alexander von Humboldt Foundation.

References

[1] Zh. I. Alferov, Fiz. Tekh. Poluprov. **1**, 436 (1967).
[2] Zh. I. Alferov, S. V. Ivanov, P. S. Kopev, A. V. Lebedev, N. N. Ledentsov, M. V. Maximov, I. V. Sedova, T. V. Shubina, and A. A. Toropov, Superlattices and Microstructures **15**, 65 (1994).
[3] E. Gross, S. Permogorov, and A. Razbirin, J. Phys. Chem. Solids **27**, 1647 (1966).
[4] N. N. Ledentsov, I. L. Krestnikov, M. V. Maximov, S. V. Ivanov, S. L. Sorokin, P. S. Kopev, Zh. I. Alferov, D. Bimberg, and C. M. Sotomayor Torres, Appl. Phys. Lett. **69**, 1343 (1996).
[5] S. V. Ivanov, S. V. Sorokin, P. S. Kopev, J. R. Kim, H. D. Jung, and H. S. Park, J. Cryst. Growth **159**, 1 (1996).
[6] N. N. Ledentsov, I. L. Krestnikov, M. V. Maximov, S. V. Ivanov, S. L. Sorokin, P. S. Kopev, Zh. I. Alferov, D. Bimberg, and C. M. Sotomayor Torres, Appl. Phys. Lett. **70**, 2766 (1997).
[7] M. V. Belousov, N. N. Ledentsov, M. V. Maximov, P. D. Wang, I. N. Yassievich, N. N. Faleev, I. A. Kozin, V. M. Ustinov, P. S. Kopev, and C. M. Sotomayor Torres, Phys. Rev. B **51**, 14346 (1995).
[8] R. Dahmani, L. Salamanca-Riba, N. V. Nguyen, D. Chandler-Horowitz, and B. T. Jonker, J. Appl. Phys. **76**, 514 (1994).
[9] E. L. Ivchenko, A. V. Kavokin, V. P. Kochereshko, P. S. Kopev, and N. N. Ledentsov, Superlattices and Microstructures **12**, 317 (1992).
[10] G. Bastard, Wave Mechanics Applied to Semiconductor Heterostructures, Les Editions de Physique, Paris 1988.
[11] C. Benoit à la Guillaume, J. M. Denber, and F. Salvan, Phys. Rev. **177**, 567 (1969).
[12] J. Ding, M. Hagerott, P. Kelkar, A. V. Nurmikko, D. C. Grillo, L. He, J. Han, and R. L. Gunshor, Phys. Rev. B **50**, 5758 (1994).
[13] K. Kondo, M. Ukita, H. Yoshida, Y. Kishida, H. Okuyama, S. Ito, T. Ohata, K. Nakano, and A. Ishibashi, J. Appl. Phys. **76**, 2621 (1994).
[14] D. Bimberg, N. Kirstaedter, N. N. Ledentsov, Zh. I. Alferov, P. S. Kopev, and V. M. Ustinov, IEEE J. Selected Topics Quantum Electronics **3**, 196 (1997).